Computed Laminography System with Various Scanning Configurations for Nondestructive Testing

Miran Park[1], Ho Kyunh Kim[2], Seungryong Cho[1]
[1] Department of Nuclear and Quantum Engineering, KAIST, South Korea
[2] School of Mechanical Engineering, Busan National University, Busan, South Korea

Introduction

- A compressive sensing (CS)-inspired image reconstruction (IR) algorithm exploits the sparsity of objective function and has shown its potential to exactly recover the images from sparse-view data in x-ray computed tomography [1]. Whereas, conventional algorithms such as Feldkamp, Davis, and Kress (FDK) algorithm result in streak artifacts due to limited sampling rate. Recent improvements in convergence speed and in minimization of controlling parameters in the CS-inspired IR algorithms increases their practical utility for clinical and industrial scanners [2].
- We have recently proposed various sparse sampling schemes for x-ray tomographic imaging and analyzed the sampling schemes by use of sampling density and data incoherence [3, 4]. However, the performance of scanning schemes at various data sparsity conditions have not been investigated yet.
- Therefore, in this work we exploited the effects of data correlation and sampling density on image quality at various sparsely sampled data conditions. For detailed comparison, we implemented an oblique computed tomography (CT) and spherical sinusoidal scanning scheme as shown in Fig. 1(a) and Fig. 1(b), respectively. Spherical sinusoidal scanning scheme is a novel scanning geometry proposed in our previous work [4], where the x-ray source-to-rotation-axis distance varies sinusoidally during a scan.

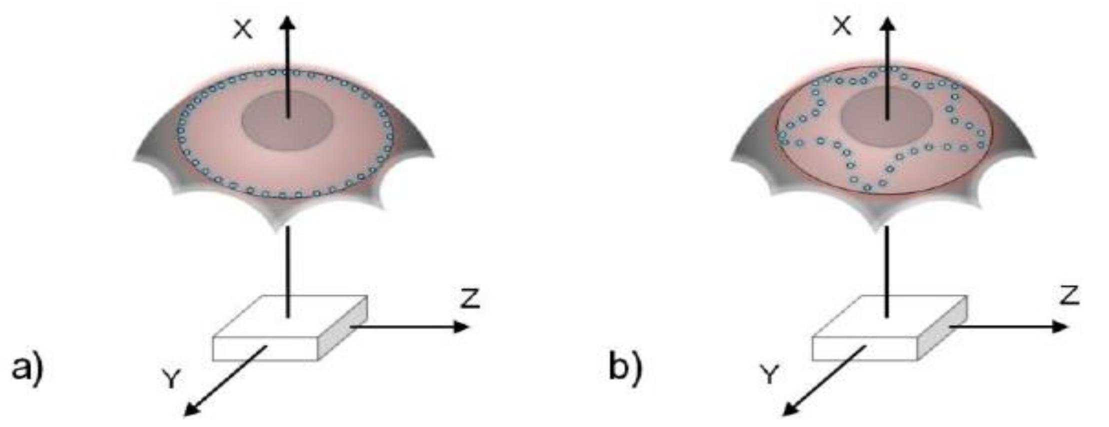

Fig. 1 Schematic illustration of oblique and spherical sinusoidal scanning configurations in 3D Cartesian coordinate.

Method

- We implemented a TV minimization algorithm, for both of the CL scanning schemes, that was originally developed by Sidky et al. [1] for a circular cone-beam CT. The objective of the TV minimization algorithm is to minimize the l_1-norm of image gradient magnitude. The solution of the optimization problem $\hat{\vec{x}}$ is defined as below:

$$\hat{\vec{x}} = argmin\|\vec{x}\|_{TV} \;\; s.t. \;\; [\![A\vec{x} - \vec{g}]\!] < \delta$$

where $\vec{x}$ is the image under reconstruction and A is the system matrix that describes the ray integrals. $\vec{g}$ represents the actual measurement and ε is the error bound, which can be determined empirically by algebraic reconstruction technique.

- In this work, the source was tilted to an angle of 30 degrees in both of the CL scanning schemes. Additionally, in case of the spherical sinusoidal scanning scheme, the source-to-rotation-axis angle was varied sinusoidally from 5 degrees to 30 degrees.
- A numerical resolution test phantom that is similar to the one used in our previous work [4] was utilized. We acquired sparse-view data sets at 24, 40, 90, 180, and 360 views on regular intervals.
- For feasibility study with real data, we acquired the data using oblique and Spherical sinusoidal scan with our benchtop system. For two oblique scans, the tilt angles were set in 30 degree and 20 degree, respectively. For sinusoidal scan, the maximum tilt angle and minimum tilt angle were 30 and 10 respectively, and it had 5 cycles.
- The laminography benchtop system is shown in figure 2. The rotation stage is held by the tilt motor, and can tilt in a certain angle. In scanning system, the source and detector are stationary while the object is tilting or rotating in a way that can produce such a scanning geometry in the object-fixed coordinates.

Fig. 2 Laminography benchtop system.

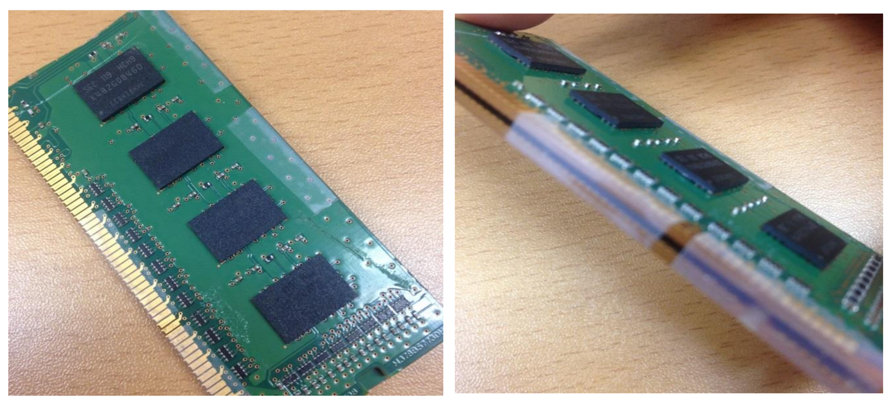

Fig. 3 The scanned object for laminography scanning test. A stacked set of RAM cards was used.

Result

- The reconstructed images of resolution-test phantom from the data acquired by both scanning schemes at 360 views are shown in Fig. 4(b). Both images are similar to each other and comparable to the reference image in Fig. 4(a). Interestingly, one can notice in Fig.4 (c) to Fig. 4(f) that image quality gradually decreases in terms of image contrast; particularly, more degraded in case of oblique CT than in spherical sinusoidal scanning scheme.

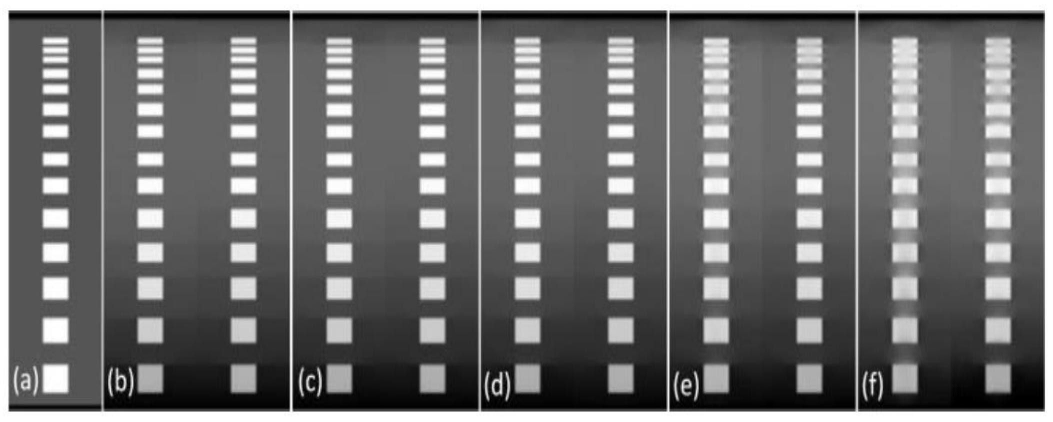

Fig. 4 Reconstructed images of resolution-test phantom: (a) ground truth and (b)~(f) are the set of images reconstructed by oblique CT (left) and spherical sinusoidal scheme (right) from data sets from 360, 180, 90, 40, and 24 views, respectively.

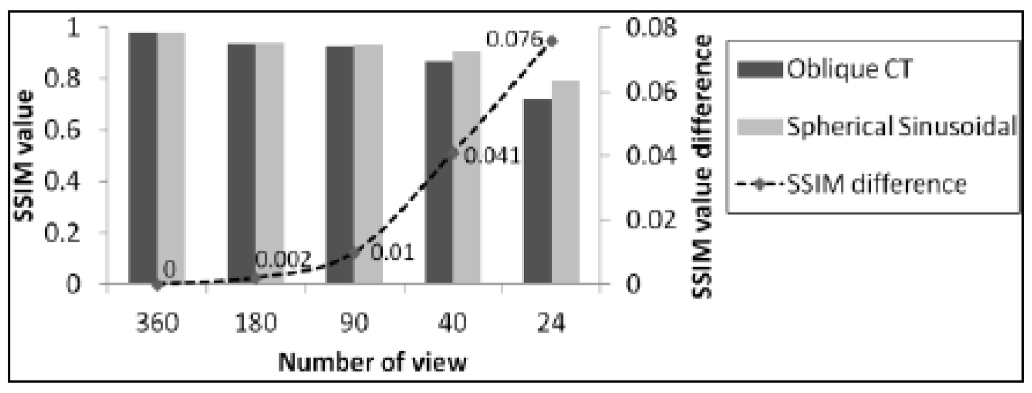

Fig. 5 Schematic illustration of data correlation in sampled data.

- In figure 6, there are the reconstructed images, which are along the depth direction , with oblique and spherical sinusoidal scan using 20 view-projections. Even if the solder balls can be detected, their shapes are elongated and distorted. However the spherical sinusoidal scan, produced slightly higher contrast of the solder balls. Higher contrast of the image is observed in the line-profile of spherical sinusoidal scan.

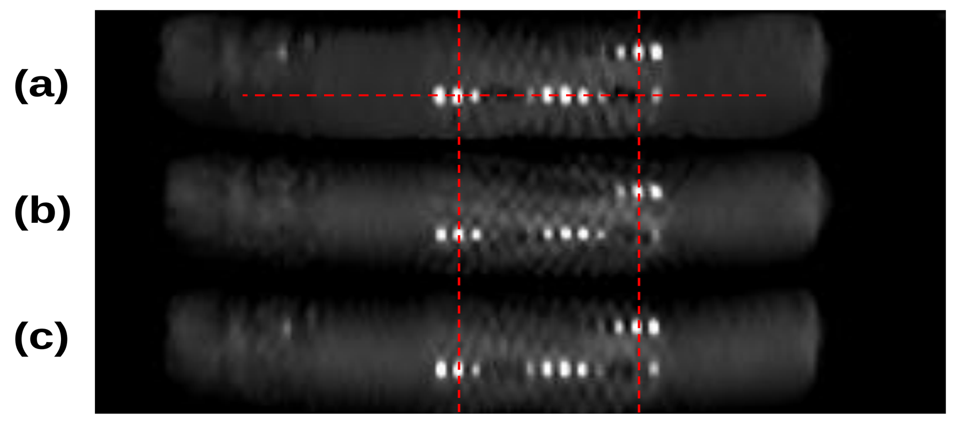

Fig. 6 Depth slice image through reconstructed image. (a) spherical sinusoidal scan (b) oblique scan tilted at 30 degree (c) oblique scan tilted at 20 degree scan

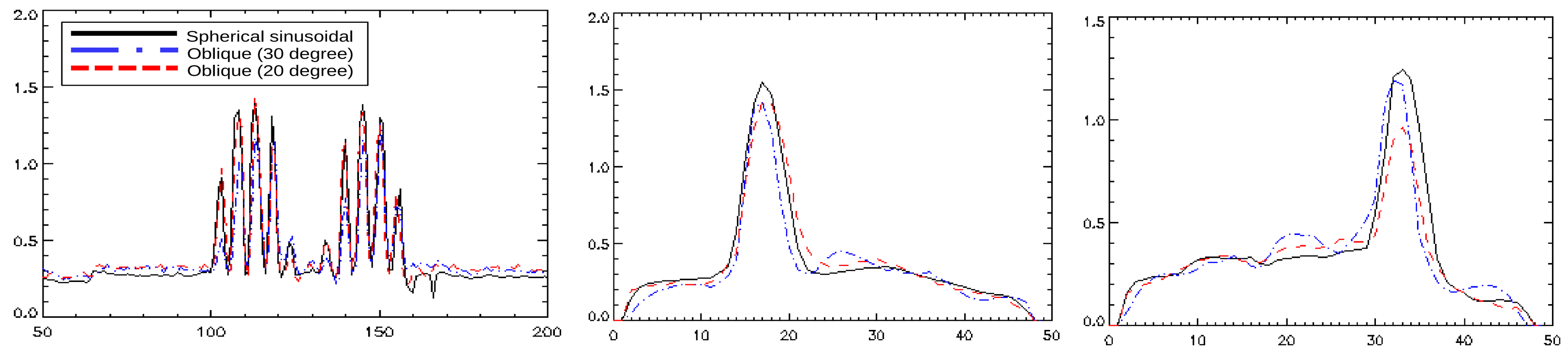

Fig. 7 The line profiles of horizontal red dotted line(left) and vertical red dotted line (middle and right) of figure 7 which indicate depth direction. The spherical sinusoidal (black solid line) has higher contrast than other scanning configuration.

Discussion

- To explain the effects of data incoherence in a sparse-view CS- framework, we considered densely and sparsely sampled cases of both scanning schemes. As one can see in Fig. 8, the source trajectory circumference corresponding to the same scanning angle is larger in the case of spherical sinusoidal scanning scheme. The number of gray pixels represents implicitly the data correlation in the sampled data.
- The difference in SSIM values increases drastically as the number of views decreases. It is believed that increase in difference of SSIM values is mainly due to the effect of data correlation and partially due to sampling density.

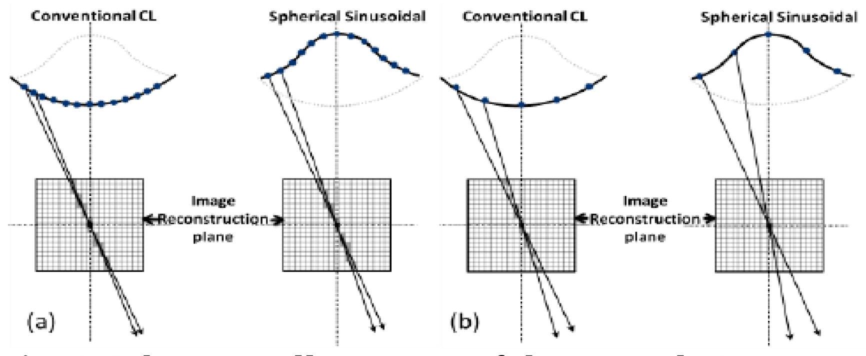

Fig. 8 Schematic illustration of data correlation in sampled data.

Table. 1 SSIM index values of the reconstructed images at various spherical sinusoidal scanning scheme's parameters.

Tilt angles	SSIM values	Frequency (/turn)	SSIM values
5	0.910	3	0.934
10	0.898	6	0.936
15	0.882	9	0.939
20	0.881	12	0.940

Conclusions

- In this paper, we investigated the effect of data correlation on image quality at various sparsely sampled projection data sets in a CS-inspired image reconstruction framework. The spherical sinusoidal scanning scheme outperforms the oblique CT in terms of image contrast, particularly when the sparsity or the insufficiency of the sampled data is high.
- Performance of the CS-inspired IR algorithms in terms of image quality can be improved if the scanning schemes are devised with a strategy that they provide least correlated data in a given data sparsity condition.

Acknowledgement

This work was funded by the National Research Foundation of Korea funded by the Ministry of Science, ICT & Future Planning NRF-2013M2A2A9043476.

References

1. E.Y. Sidky and X. Pan, "Image reconstruction in circular cone-beam computed tomography by constrained, total-variation minimization," Phys. Med. Biol., 2008, 53, (17), pp. 4777-4807, doi:10.1088/0031-9155/53/17/021

2. E. Y. Sidky, J. H. Jørgensen, and X. Pan, "Convex optimization problem prototyping for image reconstruction in computed tomography with the Chambolle-Pock algorithm," Phys. Med. Biol., 2102, 57, (10), pp. 3065-3091, doi: 0.1088/0031-9155/57/10/3065

3. S. Abbas, T. Lee, S. Shin, R. Lee, and S. Cho, "Effects of sparse sampling schemes on image quality in low-dose CT," Med. Phys., 2013, 40, (11), pp. 111915-1-111915-12, doi: 10.1118/1.4825096

4. S. Abbas, M. Park, J. Min, H. K. Kim, and S. Cho, "Sparse-view computed laminography with a spherical sinusoidal scan for nondestructive testing," Opt. Express, 2014, 22, (2) , pp. 17745-17755, doi:10.1364/OE.22.017745

5. Z. Wang, A. C. Bovik, H. R. Sheikh, and E. P. Simoncelli, "Image quality assessment: From error visibility to structural similarity," IEEE Trans. Image Process., 2004, 13, (4), pp. 600-612, doi: 10.1109/TIP.2003. 819861

Contact : Seungryong Cho, KAIST (email: scho@kaist.ac.kr) Medical Imaging & Radiotherapeutics Lab. **2016 CT Meeting**